Riekenberg, P.M.; van der Meer, M.T.J. & Schouten, S. (2020). Practical considerations for improved reliability and precision during determination of $\delta^{15}N$ values in amino acids using a single combined oxidation-reduction reactor. *Rapid Communications in Mass Spectrometry*, 34, e8797

Published version: https://doi.org/10.1002/rcm.8797

NIOZ Repository: http://imis.nioz.nl/imis.php?module=ref&refid=325506

[Article begins on next page]

Riekenberg Philip M. (Orcid ID: 0000-0002-6275-5762)

Practical considerations for improved reliability and precision during determination of $\delta^{15}N$ values in amino acids using a single combined oxidation-reduction reactor.

Philip M. Riekenberg[1]*, Marcel van der Meer[1], Stefan Schouten[1,2]

[1]NIOZ Royal Netherlands Institute for Sea Research, Marine Microbiology and Biogeochemistry Department, and Utrecht University, PO Box 59, 1790AB Den Burg, Netherlands

[2]Faculty of Geosciences, Utrecht University, PO Box 80.021, 3508TA Utrecht, Netherlands

* Author for Correspondence: phrieken@gmail.com

This article has been accepted for publication and undergone full peer review but has not been through the copyediting, typesetting, pagination and proofreading process which may lead to differences between this version and the Version of Record. Please cite this article as doi: 10.1002/rcm.8797

Abstract

RATIONALE There has been increased interest in the measurement of $\delta^{15}N$ values in amino acids to gain simultaneous insight into both trophic relationships and the composition of biogeochemical sources utilized by producers at the base of the foodweb. A new combustion reactor design in gas chromatography combustion isotope ratio mass spectrometry equipment has brought to light variable outcomes in performance, highlighting the need for better information about best practices for new systems.

METHODS Precision for $\delta^{15}N$ values in amino acids using the single combined oxidation-reduction reactor is improved across a sequence of analyses if the reactor is oxidized for a substantial period (2 h) and subsequently maintained throughout the sequence with 12-17 s seed oxidation prior to each run during gas chromatography-combustion isotope ratio mass spectrometry. A five point calibration curve using amino acids with a range of $\delta^{15}N$ values from -2.4‰ to +61.5‰ was used in combination with a 13-15 amino acid mixture to consistently normalize measurements to internationally calibrated reference materials.

RESULTS. Combining this oxidation method with normalization techniques using both internal and external standards provided a reliable throughput of ~25 samples per week. It allowed for a reproducible level of precision of $<\pm 0.5$‰, n=10 within a derivatized standard mixture across each sequence and an average sample precision of ±0.27‰ n=3, which is lower than the analytical precision typically associated with $\delta^{15}N$ values for amino acid analysis ($<\pm 1$‰).

CONCLUSIONS A few practical considerations regarding oxidation and conditioning of the combustion reactor allow for increased sequence capacity with the single combined oxidation-reduction reactor. These considerations combined with normalization techniques result in a higher throughput and reduced analytical error during the measurement of $\delta^{15}N$ values in amino acids.

Running head: Practical improvements for analysis of $\delta^{15}N$ values in amino acids

Introduction

There is increasing interest from ecologists, physiologists, archaeologists and paleoceanographers in the additional information that trophic and source amino acid $\delta^{15}N$ values can provide to further clarify poorly characterized resource contributions that often arise while measuring bulk $\delta^{13}C$ and $\delta^{15}N$ values in ecosystem research[1-5]. Difficulties can arise when variability in the underlying $\delta^{15}N$ values for resources supporting primary producers is poorly constrained or not possible to reconstruct (e.g. historical ecology) for an ecosystem. Shifts in underlying basal resource $\delta^{15}N$ values make it impossible to disentangle changes in trophic position and source mixing in systems without additional information about primary producers. However, determination of $\delta^{15}N$ values from protein-derived amino acids has allowed for the classification of amino acids into source and trophic groups providing additional information about the underlying isotopic composition of the N sources being utilized within the ecosystem as well as refining estimates for trophic position (TP) that is not available from traditional bulk measurement of $\delta^{15}N$ values[6].

Source amino acids undergo little to no isotopic fractionation during metabolism due to minimal exchange with the metabolic amino acid pool[7] leaving amino acids $\delta^{15}N$ values that largely reflect the isotopic composition of the N sources within the environment where the animal resided as the tissue was formed[8-10]. Trophic amino acids undergo considerable isotopic fractionation as they are metabolized via transamination[11] resulting in an apparent stepwise increase of $\delta^{15}N$ values that corresponds to the trophic level of the animal[11,12]. The difference in $\delta^{15}N$ value between source and trophic amino acids can thus be used to calculate trophic position (TP), a baseline-normalized estimate of the trophic level of that individual within the local food web. It is common to use either the $\delta^{15}N$ values of glutamic acid (Glu) as a trophic amino acid and phenylalanine (Phe) as a source amino acid[1,4,6,9] or a combination of several trophic and source AAs[11,12]. Increasing stepwise differences occur between trophic and source AAs in animals that correspond to trophic position[4,6,12,13]. These incremental differences between trophic positions allow for quantification of 1) the trophic discrimination factor (TDF), the per mil differences between trophic positions within an ecosystem, and 2) β, the per mil difference between the $\delta^{15}N$ values of trophic and source AAs in primary producers. Error values associated with TDF ($\pm$2.5‰)[13] and β ($\pm$0.9‰)[4] are considerably larger than or comparable with the currently accepted measurement error ($<\pm$1‰) for $\delta^{15}N$-AA analysis[14].

Measurement of $\delta^{15}N$ values of amino acids occurs generally via gas chromatography combustion isotope ratio mass spectrometry (GC/C-irMS) and requires three steps to isolate and prepare samples for analysis: 1) release of free and bound amino acids from a tissue, 2) isolation of AAs from contaminating matrix materials, and 3) derivatization to make the AAs amenable to interaction with the chromatography column for separation[1]. Acid hydrolysis of proteinaceous tissue generally occurs through heating sample material in a strong acid to 100-150°C for 1.5-10 h, thereby breaking peptide bonds and releasing the individual AAs from the proteins contained in sample material[15]. Isolation of AAs from interfering sample material is performed if samples contain a complex matrix (e.g. bone, sediment, carbonates) that can interfere with analysis and is commonly performed using cation-exchange chromatography[10,16]. Use of a cation exchange resin generally results in minimal isotopic fractionation of AAs and provides sufficient recovery of sample material to allow analysis[17]. Prior to analysis, derivatization of the AAs is required to reduce polarity and increase volatilization of the compounds. Derivatization allows for increased chromatographic separation and several derivatization agents can be used to prepare AAs for analysis e.g. trifluoroacetyl-isopropyl ester[18,19]; pentafluoropropyl isopropyl esters[20]; pivaloyl-isopropyl ester[6]; or methoxycarbonyl AA ester[21]. The derivatization agent used depends on the application, and the choice of agent should be explored with consideration towards target amino acids, whether $\delta^{13}C$ or $\delta^{15}N$ values are desired, the relative stability of the derivatized compounds, and whether introduction of halogenated compounds during GC/C-irMS is necessary[1,14].

Once the isolated and derivatized AAs are obtained, they are analyzed via GC/C-irMS through column separation of the AAs followed by combustion and then reduction. A traditional GC combustion/reduction interface for isotope ratio mass spectrometry (irMS) utilizes two reactors: first a Cu/NiO/Pt oxidation reactor heated to 950-1000°C that allows for combustion, followed by a Cu reduction reactor (550-650°C) primarily to reduce NO_x products produced during combustion. Common problems encountered during the determination of $\delta^{15}N$ values for AAs via the two separate reactor system include considerable overloading of AA carbon on the GC column as well as the combustion reactor, incomplete combustion, incomplete reduction, leakage (high background N_2), and issues with standardization to correct for drift (increasing $\delta^{15}N$ value) occurring across runs. Overloading of AA carbon during analysis of $\delta^{15}N$ values is expected as there is ~18× more carbon

produced to obtain N_2 for AA analysis (~9× more C than N in AAs and 2 AAs usually required to produce N_2). Therefore, a considerable mass of AAs must be loaded during GC/C-irMS studies in order to produce adequate N sample peaks for analysis. Consistent carbon overloading leads to relatively quick degradation of peak shape from the pre-column, quicker degeneration/clogging of the combustion reactor, and the requirement for more frequent oxidation (and ultimately replacement) of the reactor to maintain combustion capacity. Incomplete reduction results in the appearance of considerable mass 30 signal (*m/z* 30, Figure 1A) derived from the formation of NO_x, and regularly occurs after the oxidation periods (<2 min to >60 min) that are required to recover reactor combustion capacity. Leakage within the gas chromatograph is also a routine problem due to development of leaks in connections during repeated heating cycles and results in regular downtime. Proper standardization across daily sequences is important to correct for drift in $\delta^{15}N$ values that can occur as the oxidation state of the combustion reactor changes across the day.

The combined effect of these difficulties results in a low sample throughput while ecological studies examining stable isotopes often involve large sample sizes for a number of species within food webs (e.g. Christianen et al[22]). A combined oxidation/reduction reactor is now routinely used for analysis that contains a nickel oxide tube with CuO/NiO/Pt wires[14,23]. Here we discuss the optimization of the combined oxidation/reduction reactor system for the determination of $\delta^{15}N$ values of N-pivaloyl-amino acid- i-propyl esters through incorporation of a few practical changes to the daily sequence of analysis (e.g. length of seed oxidation, daily oxidation period of 2 h, and targeted loading concentrations for both standards and samples). In addition, we optimized the performance of the oxidation-reduction reactor by examining the relationship between peak areas and $\delta^{15}N$ values while incrementally increasing the seed oxidation length (7s to 22s). After the optimization of oxidation conditions during analysis, we were able to considerably increase sample throughput while achieving increased precision for the determination of $\delta^{15}N$ values of individual AAs.

Materials

Reagents and reference materials

Individual amino acids (L- form, >98% purity) were purchased (Sigma Aldrich, Darmstadt, Germany and Arndt Schimmelmann, Indiana University, Bloomington, IN, USA, respectively) and reference standard mixtures were created in house. A mix of five amino acids with a known large range in $\delta^{15}N$ values (-2.4‰ to 61.5‰; Supplementary Table 1, supporting information) and the internal reference standard L-norleucine (Nle) was used for scale normalization, and will be referred to as the 'scaling AA mix'. This mixture consisted of approximately equimolar quantities of alanine (Ala), glutamic acid (Glu), glycine (Gly, USGS65; USGS, Reston, VA, USA), phenylalanine (Phe), Nle, and valine (Val, USGS74) prepared in 0.1M HCl to a concentration of ~44 mM. A second mixture of 14 amino acids and the internal reference standard (Nle) was used as a reference standard to calculate offsets occurring during derivatization and combustion during analysis and will be referred to as the 'offset AA mix'. This standard consisted of approximately equimolar quantities of Ala, aspartic acid (Asp), Glu, Gly, leucine (Leu), lysine (Lys), isoleucine (Ile), methionine (Met), Phe, threonine (Thr), tyrosine (Tyr), serine (Ser) and Val prepared in 0.1 M HCl to a concentration of ~8.8 mM. The $\delta^{15}N$ value for each amino acid used in this mixture was established via direct measurements using an elemental analyzer isotope ratio mass spectrometry (EA-irMS) (Supplementary Table 1, supporting information). An internal reference spike of L-Nle for inclusion into samples after acid hydrolysis was prepared at 44.8 mM in 0.1M HCl. All three solutions were stored in the dark at -20°C.

The solvents and reagents for acid hydrolysis and derivatization included acetyl chloride (>99%, Fluka) , bi-distilled water, hydrochloric acid (VWR International, Boxmeer, Netherlands), magnesium sulfate (99.5% min, anhydrous; Alfa Aesar, Waltham, MA, USA), trimethylacetyl chloride (>98%; Alfa Aesar) and HPLC-grade dichloromethane (DCM), ethyl acetate, hexane, isopropanol, and methanol (Promochem, Berlin, Germany).

Sample Materials

Sample materials analyzed included muscle tissue from brown shrimp (*Crangon crangon*), green crab (*Carcinus maenas*), European bass (*Discentrarchus labrax*), blue mussel (*Mytilus edulis*), Pacific oyster (*Crassostrea gigas*), European plaice (*Pleuronectes platessa*), and harbour porpoise (*Phocoena phocoena*) collected from the Wadden Sea.

Whole body tissue excluding the gut was utilized for ragworm (*Hediste diversicolor*) and plankton (<200 µm mesh, filtered seawater) was sampled from the water column of the sublittoral zone at the Marsdiep, Netherlands (N 53° 0' 13", E 4° 46' 26"). The plankton sample was a mixture of detritus, zooplankton and phytoplankton, but was dominated by large microalgae confirmed by light microscopy and a bulk $\delta^{13}C$ value of -21.2‰. All samples excluding harbor porpoise and plankton were collected as part of the synoptic intertidal benthic surveys (SIBES) in 2011 to 2013 using the same methods as presented in Christianen et al[22]. Materials were freeze dried for 48 h and homogenized prior to analysis. The samples reflect a cross section of the Wadden Sea food web with representatives from several trophic positions including primary producer, primary consumer, omnivore, and apex predator[22].

Procedure

Amino acid isolation and preparation

3-5 mg of freeze dried, ground and homogenized tissue was acid hydrolyzed (100°C) for 10-12 h and subsequently filtered (0.45µm), lipid extracted, and spiked with the internal reference standard Nle following the sample protocol presented in Svensson et al[24] and Chikaraishi et al[4]. The hydrolysates were subsequently evaporated under N_2 gas to dryness and then isopropylated with a mixture of isopropanol and acetyl chloride (3/2, v/v) heated to 100°C for two hours (heating block set at 124°C with an independent thermometer set into a reaction vial to confirm internal reaction temperature). The hydrolysate was then evaporated to dryness (40°C, using N_2), had a hexane and dichloromethane mixture (3/2, v/v) added, and was evaporated to dryness (40°C, using N_2) twice to remove any remaining reagent. The AA *i*-propyl esters were then acylated using a mixture of trimethylacetyl chloride and DCM (1/4,v/v) by heating to 100°C for 2 h to form N-pivaloyl-amino acid- i-propyl esters. The prepared esters are volatile at this point and were allowed to evaporate to dryness at 40°C under a gentle stream of N_2, had a hexane and dichloromethane mixture (3/2, v/v) added and were then evaporated to dryness (40°C, using N_2) twice to remove any remaining reagent. The dried material was then solvent extracted using bi-distilled water and a hexane/DCM mixture (3/2, v/v) with the solvent gently evaporated to dryness (40°C, using N_2). The N-pivaloyl-amino acid- i-propyl esters were stored frozen (-20°C) and re-suspended in ethyl

acetate prior to analysis. Prepared N-pivaloyl-amino acid- i-propyl esters extracts have an expected storage capacity of <12 weeks[25] and all samples in this study were analyzed within one month of being derivatized. Additional details are provided in Supplementary material 1 (supporting information).

Analysis via GC/C-irMS

Analyses were performed using a Thermo Trace 1310 gas chromatograph connected to a Delta V Advantage irMS instrument via a GC IsoLink II combustion interface (all supplied by Thermo Fisher Scientific, Bremen, Germany) using the ramp schedule and materials detailed in Supplementary material 1 (supporting information). This analysis utilizes an oxidation-reduction reactor consisting of a NiO tube containing CuO/NiO/Pt wires within an aluminum oxide tube continuously heated to 1000°C during operation. The oxidation capacity of the reactor was ensured prior to each sequence by oxidation for 2 h, followed by a backflush period (30 min) to clear any unwanted oxidation products (NO_x monitored on *m/z* 30). During day to day analysis a sequence of 25 runs was used consisting of 5 samples run in duplicate, 2 'scaling mix' standards, 10 'offset AA mix' standards, and an alkane mix run immediately after the long daily oxidation. During the oxidation optimization, a sequence of 16 runs was used consisting of 2 samples run in triplicate with 2 'scaling AA mix', 7 'offset AA mix' standards, and an alkane mix run immediately after the long daily oxidation. Throughout both sequences, the "offset AA mix" bookends sample duplicates or triplicates. The combustion reactor was conditioned after oxidation by a single injection of alkanes suspended in ethyl acetate (~equimolar quantities of C_{17}, pristane, C_{18}, C_{20}, C_{28}, C_{30}, and C_{32}; ~25 ng uL^{-1}) and the oxidation capacity was maintained throughout the sequence by a seed oxidation (12 -17s) prior to each run during the sequence. Flow rates (GC column + backflush flows, GC column flow, and GC column + backflush + oxygen flows) measured via an internal flow meter and free O_2 (monitored at *m/z* 32) were closely monitored between sequences as indicators of declining reactor oxidation capacity or potential blockage across the lifetime of the reactor. Using this oxidation program, *m/z* 30 was held to acceptable levels that did not interfere significantly with $\delta^{15}N$ values across the run (standard deviation $<\pm 0.5‰$ for 13 AAs across 10 runs of the internal AA standard mix in each sequence) and remained relatively low across sequences (*m/z* 30 < 700 mV, ratio of *m/z* 30 / *m/z* 28 ~5%).

To prevent interference with the measurement of N_2 in the source, CO_2 was removed post combustion by a liquid N_2 trap. CO_2 was emptied from the trap prior to the 2 h oxidation

and the capillary remained outside the trap until after conditioning with *n*-alkanes was finished. As long as overloading of sample concentration did not occur, there was sufficient capacity within the CO_2 trap to hold CO_2 across the entire sequence of 25 runs without emptying. To avoid overloading of the column and CO_2 trap, all samples were first run on a GC- flame ionization detector to identify the relative amount of C contained in the samples in order to target sample dilutions prior to analysis via GC/C-irMS

Data Analysis and Normalization

The $\delta^{15}N$ values of underivatized amino acids included in standard mixes for normalization of GC/C-irMS data were determined by EA-irMS (EA-δ^{15}NAA; Supplementary Table 1, supporting information). Multiple analyses of each amino acid were performed on a Flash 2000 elemental analyzer connected to a Delta V Advantage irMS instrument via a Conflo IV interface (all from Thermo Fisher Scientific) and were calibrated using the secondary reference materials acetanilide #1 and urea #2 ($\delta^{15}N$ values of 1.18 ± 0.02‰ and 20.17 ± 0.06‰, respectively) which were calibrated on IAEA-N-1 and IAEA-N-2[26]. The precision for this analysis is ±0.1‰.

Derivatized samples are routinely analyzed in duplicate during GC/C-irMS, but during the oxidation optimization process in October 2019, the samples were analyzed in triplicate. Normalization and scaling for samples and standards followed the calculations presented in Yarnes and Herszage[14] and were applied to each sequence. This method uses a set of three corrections to normalize the data produced through use of 1) an internal reference spike (Nle) included in all samples and standard mixtures and that undergoes the same derivatization, combustion, and reduction process, 2) an amino acid mixture used to calculate an offset for each individual amino acid resulting from derivatization, and 3) a scaling standard mixture using amino acids with a large range of $\delta^{15}N$ values calibrated against international standards. First, all samples and standard mixtures were evaluated against the internal reference spike instead of the laboratory reference monitoring gas due to the principle of identical treatment. Subsequently, a corrected value ($\delta^{15}NAA_{Off}$) that accounted for derivatization was calculated for all 13-14AAs in the reference mixtures using the equation:

1) $\delta^{15}NAA_{Off}$ = measured δ^{15}NAA - $\delta^{15}NAA_i$

where $\delta^{15}NAA_i$ = measured $\delta^{15}NAA$ – known $\delta^{15}NAA$ for each of the amino acids in the 13 AA mixture. The $\delta^{15}NAA_{Off}$ values were then normalized to international reference standards by performing a linear regression of the measured $\delta^{15}NAA_{Off}$ values and the known values of the 'scaling AA mix' and using the resulting equation to correct the offset adjusted sample values to an internationally calibrated scale across all 5 AAs included in the 'scaling AA mix' as:

2) $\delta^{15}NAA_{scaling} = m * \delta^{15}NAA_{Off} + b$

where m is the slope and b is the intercept of the regression across all 5 AAs. The materials used for each correction are 1) Nle, 2) 'offset AA mix, and 3) 'scaling AA mix' ($\delta^{15}N$ values ranging from -2.4‰ to +61.5‰; Ala, Glu, Gly, Phe, and Val; Arndt Schimmelmann, Indiana University, Bloomington, IN, USA). The $\delta^{15}N$ values are all presented as 'per mil' (‰) relative to atmospheric nitrogen as determined by the International Atomic Energy Agency (IAEA, Vienna, Austria).

Statistics

In each sequence samples and 'scaling AA mix' were run in duplicate. 'Offset AA mix' values are reported as mean ± standard deviation across each sequence (n=10). Linear regressions were used to calculate the scaling corrections to internationally calibrated standards (see above). The separation index was calculated as:

3) $Rt_2 - Rt_1 / 0.5 \times (W_1 + W_2)$

where Rt is the retention time and W is the width for each of peaks being compared. TP estimates were made using normalized measurements for Glu and Phe within individual samples and calculated as:

4) $TP = 1 + (\delta^{15}N_{Glu} - \delta^{15}N_{Phe} - \beta) / TDF_{Glu\text{-}Phe}$

where $\delta^{15}N_{Glu}$ and $\delta^{15}N_{Phe}$ are the $\delta^{15}N$ values for Glu and Phe in the sample, and TDF and β are set at 7.6 ± 2.5‰ and 3.4 ± 1.5‰, respectively[4,13].

Assessment

Conditioning and monitoring of reactor performance

Our previous method for measuring the $\delta^{15}N$ values of amino acids ([24]) used separate oxidation and reduction reactors in a Thermo Fisher Scientific GC combustion III system. In this current method, oxidation by flushing O_2 was used to improve and maintain combustion capacity only sparingly when the peak shape deteriorated (e.g. tailing, reduced peak height). This was due to the considerable increase of *m/z* 30 intensity (from NO_x) that interfered with measurement of $\delta^{15}N$ value and loss of intensity of *m/z* 28 and 29 (from N_2) that occurred after this oxidation (Figure 1A, *m/z* 30 10-50 V). After oxidation, recovery of *m/z* 29/28 required multiple injections of N-containing compounds (e.g. tributylamine, AA standard mix, n=5-20) to condition both reactors and resulted in considerable loss of analysis time to recover the measurement baseline for *m/z* 30 (0.5-2 days). Here, using the combined oxidation and reduction reactor in the Thermo Fisher Scientific IsoLink II system, it was necessary to include an extended oxidation period at the beginning of the daily sequence prior to standard and sample analysis. Daily extended oxidation resulted in predictable oxidation capacity from the reactor and *m/z* 29/28 across sequences for the two month analytical period presented here (80 samples in duplicate; 160 standards; 16 sequences). In addition, we present a quantitative optimization of oxidation performance performed directly after installation of a new reactor for routine analysis to demonstrate a procedure for establishing optimal oxidation conditions for other laboratories. These findings represent a significant improvement in precision, reliability, and laboratory throughput of $\delta^{15}N$-AA samples solely due to practical considerations built into routine analysis procedures. Subsequently, we have observed the maintenance of precision and reliability for this method across >1400 standards and 600 samples using 3 reactors with an average lifetime of ~60 sequences each.

To obtain a predictable oxidation capacity from the combined oxidation-reduction reactor, we used a combination of an extended initial oxidation, followed by conditioning via a mixture of alkanes in ethyl acetate, and subsequently maintained oxidation through a seed oxidation (7, 12, 17, and 22 seconds) after each run. This strategy has resulted in a *m/z* 30 baseline ranging from <614±63 mV during the analysis of the initial offset standard to >367 ± 25 mV during the analysis for the last 'offset AA mix' (the 25th sample in each sequence). The m30 baseline was elevated in a consistent manner across the sequence as evidenced by consistent *m/z* 29/28 and a precision <0.5‰ between the 7 to 10 'offset AA mix' standards run across each sequence. Consistent reproducibility in the *m/z* 29/28 across sequences led to a predictable interference (Figure 1B) between sequences across the lifetimes of the three oxidation/reduction reactors that we have used. In contrast, decreased combustion capacity

(caused by shorter seed oxidation times) led to incomplete conversion of the analyte and resulted in a variable increase in $\delta^{15}N$ values and loss of peak areas across sequences (~2‰ 7 and 12 second seed oxidations, peak area ratios < 1; Figure 3). Longer seed oxidation times resulted in a progressive decrease of $\delta^{15}N$ values in the standards as sequences progressed (0.7-1‰ for 22 second seed oxidation; Figure 3) and caused decreased precision. Optimized performance of the combined oxidation/reduction reactor depends on an oxidation maintenance period that supports complete conversion of the analyte with a minimal decrease of $\delta^{15}N$ values resulting from over-oxidation across the sequence (Figure 3). Once a balance between these two effects is found, the offset across each run in the *m/z* 29/28 ratio becomes relatively consistent across the sequence and allows for a stable correction for this effect through the use of the 'offset AA mix' to adjust standard values within each sequence (Figure 2A). Using this optimization for each reactor, we have successfully maintained a precision of < 0.5‰ across ~140 sequences, 700 samples, n=2), using the structure of standards (n=10, 1400 injections; Figure 2) and samples (Table 2), but we present the results for both the standards (n=7) and the samples (n=3) used during the optimization procedure for a newly installed reactor (Figure 3; Supplementary Tables 2 and 3, supporting information). We recognize that reactors behave differently and will potentially need to undergo optimization depending on the variance in the combustion capacity, but have found that decreasing standard precision (>0.5‰) and peak areas across sequences are the key symptoms to monitor deteriorating reactor conditions.

This performance appears to be little changed during short-term analysis with shortening of the 2 h daily oxidations. The 30 min backflush following this oxidation appears to be sufficient to return the *m/z* 28/29 to baseline before analysis of standards regardless of whether a 30 min or 2 h oxidation was used. When using the shorter oxidation period, we did observe small peaks <200 mV occurring during the analysis of the alkane mixture probably from incompletely combusted analyte remaining in the reactor, but the precision for the subsequent 'offset AA mix' standards remained unaffected. We have observed similar peaks occasionally after sequences with elevated loading rates of analyte when using the 2 h oxidation, but have seen no decrease in precision within the sequences that have followed. We have chosen to continue with the daily 2 h oxidation as it has not appeared to adversely affect the reactor lifetimes and ensures that any recalcitrant material remaining in the reactor is sufficiently oxidized regularly to prevent buildup that can lead to premature failure due to clogging. We cannot speak to the reliability of longer term use of shorter oxidation periods.

In additional, we incorporated into the sequence an ISODAT (Thermo Fisher Scientific) method monitoring *m/z* 32 (O_2) with the backflush turned off between samples and standards. When the oxidation capacity of the reactor was sufficient, *m/z* 32 quickly approached 50 V, but when the oxidation capacity of the reactor was exceeded, *m/z* 32 would only register 10-30 V and the peak retention times retarded with subsequent runs (~5 seconds). Monitoring *m/z* 32 throughout the sequence allowed for within-sequence monitoring of the reactor oxidation capacity and helped to identify when overloading began to occur.

Furthermore, monitoring carrier gas flow rates prior to each sequence provided additional information about the long term state of the combustion reactor. Declining carrier gas flow rates when the backflush is turned off indicated that clogging of the reactor was beginning to occur, although there is some day to day variability in these flow rates (1.56 ± 0.18 mL min^{-1} across the lifetime of the reactor). Directly after analysis, the GC column flow was >1.4 mL min^{-1} (set at 1.6 mL min^{-1}) and the *m/z* 32 peak is >50 V with the backflush turned off. These measurements will vary between systems, but have been included to provide an example of the variation in these observations across the lifetime of reactors. We observed that failure of the reactor was characterized by a gradually decreased precision (>0.5‰) for $\delta^{15}N$ values in the 'offset AA mix' caused by the increase in standard $\delta^{15}N$ values and lower peak area ratios (Figure 3) towards the end of sequences. This gradual degradation requires standards to be run throughout the sequence to characterize how the oxidation capacity is maintained towards the end of sequence. Our experience is currently limited to the gradual failure of two reactors, and does not represent all possible outcomes for reactor failure (e.g. blockage, leakage).

Another consideration for increased reliability across a daily sequence was, prior to analysis via GC/C-irMS, to analyze samples via GC-flame ionization detector (DB-5MS, Agilent Technologies, Santa Clara, CA, USA; 60 m × 0.32 mm o.d. × 0.5 µm film thickness) in order to ensure that comparable amounts of sample are injected on column for all samples (Leu > 0.3 µg) based on the relative peak areas for sample versus the internal standard spike (Nle, ~0.3 µg, Table 1). This allowed for targeted dilution for both samples and standards prior to on-column injection during GC/C-irMS analysis that resulted in *m/z* 29 peak heights of ~300 mV (*m/z* 29 background of 15 mV) for both standards and samples (for Leu, with variations in peaks heights for other AAs depending on tissue type). Maintenance of comparable analyte loading rates allowed the CO_2 trap to remain submerged throughout a

sequence (10 'offset AA mix', 2 'scaling AA mix', and 5 samples in duplicate), eliminating any baseline disturbances resulting from the remnants from emptying the trap between runs. When high amounts of analyte are loaded on column (e.g. accidental evaporation of solvent in a sample vial) the CO_2 trap can become overloaded towards the end of the sequence. Overloading of CO_2 causes increased peak retention times, considerable drift of standard $\delta^{15}N$ values, and decreased precision between standard and sample replicates. Overloading also causes increased co-elution for Asp and Thr and for Ser and Met as the previous peaks increasingly do not come down to baseline. Baseline interferences can be further minimized through targeted loading rates if users are focused on improved accuracy for these amino acids. This method represents a generalized separation with better precision between measurements for a suite of amino acids with acknowledged co-elution potential for a subset of amino acids. Further optimization of ramp temperature, flow, and loading should be performed to allow for further separation with a 60 m DB-5 column if users are pursuing particular accuracy for specific problematic AAs. Alternatively, purification of individual AAs via HPLC with subsequent analysis via IRMS is a viable option with improved precision for these applications[27] and a direct comparison between this method and the method presented in this study would be useful to the wider community.

Normalization

Rather than using solely a single AA mixture to account for both changes in $\delta^{15}N$ values due to derivatization of AAs and long-term stability[24], we followed the approach of Yarnes and Herszage[14] which uses 3 standards to normalize AAs. These standards are: 1) a spiked AA reference standard (Nle) included in every standard and sample, 2) an AA mixture to account for changes in $\delta^{15}N$ values during derivatization 'offset AA mix'(Figure 1B), and 3) an AA mixture to scale to calibrated international standards 'scaling AA mix' (Table 1). The precision was within ±0.5‰ for both standard mixes run during the analysis period (5 weeks; 16 sequences; 'offset AA mix': 160 injections, average σ ± 0.22‰, range ± 0.18-0.25, min-max: Met-Ala; 'scaling AA mix': 32 injections, σ ±0.19, range ± 0.1-0.33, min-max: Val-Gly; Figure 1B and Table 1) as well as the optimization period in October 2019 (Figure 4; and Supplementary Tables 2 and 3, supporting information). This represents an improvement over the precision of our previously utilized standard mix (0.7-1.2‰)[24] and the commonly reported precision of ±1‰ for measurement of ^{15}N values in AAs[14,21]. Investigating the effects of each correction individually found that the difference between amino acids measured by EA-irMS and their derivatives prepared via the NPiP pathway

($\delta^{15}NAA_i$ values) was larger when only corrected to the spiked internal reference standard than for standards that were corrected to the internal reference standard and scale-normalized (1.41±0.18‰ vs -0.88±0.22‰, respectively; Figure 2). Measured differences between AAs measured via EA and their derivatives measured via GC/C-irMS were larger for some amino acids (derivatization offset AA mix: Gly, Thr, and Ser ~2‰, Figure 2; Scaling AA mix: Ala ~2.3‰, Figure 2). Samples that were corrected using this method for normalization had an average precision of 1) 0.18‰ for duplicate measurements during the initial sampling period (0.01-0.49‰ min-max, 12AAs, 7 samples; Table 2) and 2) 0.27‰ for triplicate measurements run during the oxidation optimization (0.04-0.4 8‰, 15 AAs; 2 samples; Supplementary Table 3, supporting information). All sample measurements have been normalized to internationally calibrated reference materials to ensure comparabilitywith measurements in similarly calibrated analyses.

Trophic position

In addition to the canonical source and trophic AAs (Phe, Glu), the improved method has also allowed $\delta^{15}N$ measurements for other source (Lys, Met, Ser, Tyr), trophic (Ala, Asp, Ile, Leu, Val) and other (Gly, Met, and Thr) AAs with improved precision (±0.5‰, 1σ; Figure 1B, Tables 1 and 2). Improved precision for non-canonical AAs will allow for further reduction of the variability associated with TDF for both consumers and β, as multiple amino acids are increasingly utilized to better constrain variability amongst AA types,[11,28] or alternative trophic AAs (e.g. Pro) are utilized for TP measurements[29,30]. The TPs calculated here using Glu and Phe (Eqn. 4) ranged from 1.3 ± 0.2 for a plankton sample dominated by microalgae to 3.2 ± 0.85 for *D. labrax*, which correlate well with values expected for primary producers to secondary consumers, respectively (Table 2). The error associated with the calculation of TP is primarily a result of the considerable error associated with TDF and β due to physiological variance within the metabolism of individuals and is not considerably reduced with decreased analytical error (±0.21 vs ±0.24 TP using precision ±0.5‰ and ±1‰, respectively, for phytoplankton using the error propagation formula presented in Okhouchi[1]). Examination of TDF and β within consumer-resource groups with better normalization and decreased analytical error should improve estimates below the current threshold of ±2.5‰ and ±0.9‰ as these variables better reflect physiological and taxonomic variability in biological fractionation[4,14,31]. A reduction of 1‰ in the error estimate for TDF (from 2.5‰ to 1.5‰) halves the propagated error for the TP of secondary consumers

(European Bass, ±1.1 versus ±0.4, respectively)[1]. In addition, improved instrument reliability and reduced downtime allows for increased replication within studies and better efficiency during method development for difficult materials (e.g. microphytobenthos, detrital and sediment trap organic matter).

To demonstrate typical results for the improved method, we analyzed AAs for 6 species that are relevant to our current work in the Wadden Sea: *Crangon crangon*, brown shrimp; *Dicentrarchus labrax*, European bass; *Hediste diversicolor*, Ragworm; *Mytilus edulis*, blue mussel; *Phocoena phocoena*, harbor porpoise; and *Pleuronectes platessa*, European plaice and phytoplankton sampled from the Wadden Sea (Table 2, Figure 5). These samples represent an expected range of animals from the Wadden Sea food web that spans from primary producer to apex predator (*P. phocena*). Both the highest and lowest TPs in this study (*D. labrax* and phytoplankton, respectively) demonstrated elevated $\delta^{15}N$ values for the trophic AAs in the secondary consumer compared with the primary producer. The $\delta^{15}N$ values for the source AAs were generally lower, reflecting the smaller fractionation associated with their processing during trophic transfer, with the notable exception of Thr, which was considerably ^{15}N-depleted for the European bass (-1.4‰; Table 2). This negative correlation with elevated trophic position has been previously observed[11,31,32] and may indicate a strong reverse fractionation associated with trophic transfer of N or be an effect of diet quality or metabolic rate[2,13]. The $\delta^{15}N$ value for Gly is relatively close to that of Phe (9.2‰ and 10.1‰, respectively) and may reflect a minimal contribution of microbially-degraded material to the diet of European bass[33] or may reflect routing and utilization of Gly as a source AA if Gly is sufficient in the diet[34]. This analytical method reliably produces $\delta^{15}N$ values for non-canonical AAs that should allow for further insight into the metabolic processes occurring during trophic transfer of AAs between species.

Comparison between three species, *Cerastoderma edule, Arenicola marina,* and *Macoma balthica*, using both the method presented here and the previous method (Svensson et al[24]; Figure 6) showed improved precision for Glu and TP (3.5‰ vs 2.3‰ for Glu and 0.36 vs 0.21 for TP; old vs new, respectively) but decreased precision for Phe (1.7‰ vs 1.9‰; Supplementary Table 4, supporting information). Increased variability for Phe was driven by the increased variability within *M. balthica* examined using the new method (±1.7‰, n= 8) and probably reflects regional variability in the underlying primary producers supporting this population. Samples were taken from the same sampling sites in the Wadden Sea as part of the SIBES 2011 and 2013 sampling campaigns, but do not include the same

individuals for each analysis. Decreased variability was observed primarily due to more consistent standardization techniques that better account for the drift in AA $\delta^{15}N$ values that occurred across the daily sequences largely due to interference from *m/z* 29/28. Increased analytical throughput with the new method has allowed for more routine inclusion of standards throughout the sequence for normalization than was possible or practical with the previous method. In addition, the $\delta^{15}N$ values of each individual AA has been standardized to calibrated reference materials and will be comparable with similarly standardized measurements in other laboratories. Improvement in analytical precision and more widespread utilization of normalization to international standards will allow for better comparison between TPs of animals across ecosystems.

Other Applications

Improved precision allows for finer resolution of $\delta^{15}N$ differencess within source AAs that may result in positive identification of smaller per mil shifts for basal resource utilization amongst populations[29,35]. Reduced analytical error will improve resolution of differences for source AAs in materials that are formed across an animal's lifetime such as baleen or otoliths, where resource shifts are likely to be incremental resulting in small initial ‰ changes[10]. Improved resolution will benefit the construction of isoscapes, detailed mapping of isotope baselines for individual compounds across landscapes, allowing for finer partitioning of regional differences in examined source AAs[36,37]. Decreased analytical error will improve resolution for equations utilizing multiple individual AA values (e.g. such as ΣV, an estimate of the amount of microbial re-synthesis of AAs that potentially indicates reworking of detrital material within the ecosystem[18, 1]). Finally, improved analytical precision and wider use of compound-specific normalization to available international standards will decrease the variance associated with AA measurements and improve between-study comparisons and meta-analyses for studies using these techniques.

LITERATURE CITED

1. Ohkouchi N, Chikaraishi Y, Close HG, et al. Advances in the application of amino acid nitrogen isotopic analysis in ecological and biogeochemical studies. *Org Geochem.* 2017;113:150-174.
2. Fuller BT, Petzke KJ. The dietary protein paradox and threonine 15N-depletion: Pyridoxal-5'-phosphate enzyme activity as a mechanism for the δ15N trophic level effect. *Rapid Commun Mass Spectrom.* 2017;31(8):705-718.

3. Li C, Jian Z, Jia G, Dang H, Wang J. Nitrogen Fixation Changes Regulated by Upper Water Structure in the South China Sea During the Last Two Glacial Cycles. *Global Biogeochemical Cycles.* 2019;33(8):1010-1025.
4. Chikaraishi Y, Ogawa NO, Kashiyama Y, et al. Determination of aquatic food-web structure based on compound-specific nitrogen isotopic composition of amino acids. *Limnology and Oceanography: Methods.* 2009;7(11):740-750.
5. McClelland JW, Montoya JP. Trophic relationships and the nitrogen isotopic composition of amino acids in plankton. *Ecology.* 2002;83(8):2173-2180.
6. Chikaraishi Y, Kashiyama Y, Ogawa NO, Kitazato H, Ohkouchi N. Metabolic control of nitrogen isotope composition of amino acids in macroalgae and gastropods implications for aquatic food web studies. *Marine Ecology Progress Series.* 2007;342:85-90.
7. O'Connell TC. 'Trophic' and 'source' amino acids in trophic estimation: a likely metabolic explanation. *Oecologia.* 2017;184(2):317-326.
8. Lorrain A, Graham BS, Popp BN, et al. Nitrogen isotopic baselines and implications for estimating foraging habitat and trophic position of yellowfin tuna in the Indian and Pacific Oceans. *Deep Sea Research Part II: Topical Studies in Oceanography.* 2015;113:188-198.
9. Vander Zanden HB, Arthur KE, Bolten AB, et al. Trophic ecology of a green turtle breeding population. *Marine Ecology Progress Series.* 2013;476:237-249.
10. Vane K, Wallsgrove NJ, Ekau W, Popp BN. Reconstructing lifetime nitrogen baselines and trophic position of Cynoscion acoupa from δ^{15}N values of amino acids in otoliths. *Marine Ecology Progress Series.* 2018;597:1-11.
11. Bradley Christina J, Wallsgrove Natalie J, Choy CA, et al. Trophic position estimates of marine teleosts using amino acid compound specific isotopic analysis. *Limnology and Oceanography: Methods.* 2015;13(9):476-493.
12. Nielsen JM, Popp BN, Winder M. Meta-analysis of amino acid stable nitrogen isotope ratios for estimating trophic position in marine organisms. *Oecologia.* 2015;178(3):631-642.
13. McMahon KW, McCarthy MD. Embracing variability in amino acid δ15N fractionation: mechanisms, implications, and applications for trophic ecology. *Ecosphere.* 2016;7(12):e01511-n/a.
14. Yarnes CT, Herszage J. The relative influence of derivatization and normalization procedures on the compound-specific stable isotope analysis of nitrogen in amino acids. *Rapid Commun Mass Spectrom.* 2017;31(8):693-704.
15. Cowie GL, Hedges JI. Improved amino acid quantification in environmental samples: charge-matched recovery standards and reduced analysis time. *Marine Chemistry.* 1992;37(3):223-238.
16. Metges CC, Petzke KJ. Measurement of15N/14N Isotopic Composition in Individual Plasma Free Amino Acids of Human Adults at Natural Abundance by Gas Chromatography–Combustion Isotope Ratio Mass Spectrometry. *Anal Biochem.* 1997;247(1):158-164.
17. Takano Y, Kashiyama Y, Ogawa NO, Chikaraishi Y, Ohkouchi N. Isolation and desalting with cation-exchange chromatography for compound-specific nitrogen isotope analysis of amino acids: application to biogeochemical samples. *Rapid Commun Mass Spectrom.* 2010;24(16):2317-2323.
18. McCarthy MD, Benner R, Lee C, Fogel ML. Amino acid nitrogen isotopic fractionation patterns as indicators of heterotrophy in plankton, particulate, and dissolved organic matter. *Geochim Cosmochim Acta.* 2007;71(19):4727-4744.
19. McCarthy MD, Lehman J, Kudela R. Compound-specific amino acid δ15N patterns in marine algae: Tracer potential for cyanobacterial vs. eukaryotic organic nitrogen sources in the ocean. *Geochim Cosmochim Acta.* 2013;103:104-120.
20. McCarthy MD, Hedges JI, Bennar R. Major bacterial contribution to marine dissolved organic nitrogen. *Science.* 1998;281(5374):231-234.

21. Walsh RG, He S, Yarnes CT. Compound-specific δ13C and δ15N analysis of amino acids: A rapid, chloroformate-based method for ecological studies. *Rapid Commun Mass Spectrom.* 2014;28(1):96-108.
22. Christianen MJA, Middelburg JJ, Holthuijsen SJ, et al. Benthic primary producers are key to sustain the Wadden Sea food web: stable carbon isotope analysis at landscape scale. *Ecology.* 2017;98(6):1498-1512.
23. Reinnicke S, Juchelka D, Steinbeiss S, Meyer A, Hilkert A, Elsner M. Gas chromatography/isotope ratio mass spectrometry of recalcitrant target compounds: performance of different combustion reactors and strategies for standardization. *Rapid Commun Mass Spectrom.* 2012;26(9):1053-1060.
24. Svensson E, Schouten S, Hopmans EC, Middelburg JJ, Sinninghe Damsté JS. Factors Controlling the Stable Nitrogen Isotopic Composition ($\delta^{15}N$) of Lipids in Marine Animals. *PLOS One.* 2016;11(1):e0146321.
25. Corr LT, Berstan R, Evershed RP. Optimisation of derivatisation procedures for the determination of δ13C values of amino acids by gas chromatography/combustion/isotope ratio mass spectrometry. *Rapid Commun Mass Spectrom.* 2007;21(23):3759-3771.
26. Schimmelmann A, Albertino A, Sauer PE, Qi H, Molinie R, Mesnard F. Nicotine, acetanilide and urea multi-level 2H-, 13C- and 15N-abundance reference materials for continuous-flow isotope ratio mass spectrometry. *Rapid Communn Mass Spectromy.* 2009;23(22):3513-3521.
27. Broek TAB, McCarthy MD. A new approach to δ15N compound-specific amino acid trophic position measurements: preparative high pressure liquid chromatography technique for purifying underivatized amino acids for stable isotope analysis. *Limnology and Oceanography: Methods.* 2014;12(12):840-852.
28. Nielsen SL, Risgaard-Petersen N, Banta GT. Nitrogen retention in coastal marine sediments—a field study of the relative importance of biological and physical removal in a danish estuary. *Estuaries and Coasts.* 2017:1-12.
29. Vokhshoori NL, McCarthy MD, Collins PW, et al. Broader foraging range of ancient short-tailed albatross populations into California coastal waters based on bulk tissue and amino acid isotope analysis. *Marine Ecology Progress Series.* 2019;610:1-13.
30. Brault EK, Koch PL, Costa DP, et al. Trophic position and foraging ecology of Ross, Weddell, and crabeater seals revealed by compound-specific isotope analysis. *Marine Ecology Progress Series.* 2019;611:1-18.
31. McMahon KW, Thorrold SR, Elsdon TS, McCarthy MD. Trophic discrimination of nitrogen stable isotopes in amino acids varies with diet quality in a marine fish. *Limnology and Oceanography.* 2015;60(3):1076-1087.
32. Hare PE, Fogel ML, Stafford Jr TW, Mitchell AD, Hoering TC. The isotopic composition of carbon and nitrogen in individual amino acids isolated from modern and fossil proteins. *Journal of Archaeological Science.* 1991;18(3):277-292.
33. Calleja ML, Batista F, Peacock M, Kudela R, McCarthy MD. Changes in compound specific $\delta^{15}N$ amino acid signatures and d/l ratios in marine dissolved organic matter induced by heterotrophic bacterial reworking. *Marine Chemistry.* 2013;149:32-44.
34. Webb EC, Lewis J, Shain A, et al. The influence of varying proportions of terrestrial and marine dietary protein on the stable carbon-isotope compositions of pig tissues from a controlled feeding experiment. *STAR: Science & Technology of Archaeological Research.* 2017;3(1):28-44.
35. Madigan DJ, Chiang WC, Wallsgrove NJ, et al. Intrinsic tracers reveal recent foraging ecology of giant Pacific bluefin tuna at their primary spawning grounds. *Marine Ecology Progress Series.* 2016;553:253-266.
36. Vokhshoori NL, McCarthy MD. Compound-specific δ15N amino acid measurements in littoral mussels in the California upwelling ecosystem: a new approach to generating baseline δ15N Isoscapes for coastal ecosystems. *Plo SOne.* 2014;9(6):e98087-e98087.

37. McMahon KW, Newsome SD. Amino Acid Isotope Analysis: A New Frontier in Studies of Animal Migration and Foraging Ecology. Chapter 7 In: Hobson KA, Wassenaar LI, eds. *Tracking Animal Migration with Stable Isotopes (Second Edition).* Academic Press; 2019:173-190.

Acknowledgements: We thank students from the 2018 NIOZ Marine Master course for providing samples for analysis. We thank Dieter Juchelka and Maria de Castro (Thermo Fisher Scientific, Bremen, Germany) for technical assistance following considerable downtime. We also thank Diane O'Brien (University of Alaska) and Christopher Yarnes (UC Davis) for encouraging output of a relatively user specific method paper during discussion at ISOECOL 2018. In addition, this work benefited from participation in the ISOECOL 2018 workshop: Approaches to improve the reproducibility of amino acid stable isotope analyses.

Table 1: Retention times and separation indices for analyzed amino acids for both individual methods as well as a comparison between the two methods. The separation index is calculated both for the amino acids present in each run and for the comparable amino acids resulting from each method. Separation index values greater than 1 indicate a difference in peak retention times that is larger than the average width of both peaks. Asp and Thr (1.1) co-eluted at higher standard concentrations, but co-elution was not often observed for peaks with separation index values greater than 1.5.

	Svensson et al[24]				This study				Comparison
	Retention Time (min)	Width (second)	Amplitude *m/z* 28 (mV)	Separation index	Retention Time (min)	Width (second)	Amplitude *m/z* 28 (mV)	Separation index	Separation index
Ala					10.4	12.3	655	2.7	
Gly	17.8	25.5	142	24.0	11.0	11.9	293	7.1	16.9
Val					12.9	14.4	589	5.8	
Leu					14.3	13.8	665	1.9	
Ile					14.8	16.3	513	3.0	
Nle	28.8	29.3	131	50.3	15.5	13.4	749	7.0	20.2
Pro					17.1	16.1	550	7.7	
Asp					18.6	10.9	488	1.1	
Thr					18.8	11.3	427	2.0	
Ser					19.2	15.5	676	1.5	
Met					19.6	14.4	864	4.3	
Glu	49.5	20.1	96	5.6	20.5	11.7	422	3.9	3.9
Phe	51.4	21.5	249	26.0	21.4	13.4	536	20.8	21.2
Lys					25.8	12.5	614	4.5	
Tyr	59.6	16.3	322		26.8	16.1	755		

Table 2: $\delta^{15}N$ values for NPiP derivatives from acid hydrolysis of tissue of different species from the Wadden Sea after normalization using both internal and scaling AA mix. Plankton was material from a bulk water sample retained using a 200 µm mesh size and predominantly consisted of large microalgae. N.D. indicates not determined as the peak heights were below 100 mV and therefore were not suitable for integration.

	Brown Shrimp	**European Bass**	**Mussel**	**European Plaice**	**Ragworm**	**Harbour Porpoise**	**Plankton**
	Crangon crangon	*Dicentrarchus labrax*	*Mytilus edulis*	*Pleuronectes platessa*	*Hediste diversicolor*	*Phocoena phocoena*	
Ala	27.31(0.28)	30.24(0.23)	19.94(0.04)	24.62(0.28)	16.40(0.26)	22.83(0.24)	12.98(0.02)
Asp	22.7(0.20)	26.65(0.26)	16.19(0.05)	23.00(0.16)	15.58(0.01)	23.36(0.15)	14.12(0.41)
Glu	27.65(0.33)	30.16(0.03)	18.26(0.20)	25.52(0.23)	18.56(0.10)	26.00(0.13)	15.79(0.29)
Gly	10.25(0.30)	9.23(0.39)	8.19(0.11)	9.85(0.29)	8.95(0.10)	20.46(0.03)	10.98(0.19)
Ile	18.8(0.30)	26.59(0.11)	18.00(0.29)	22.56(0.10)	15.52(0.08)	20.85(0.29)	10.42(0.06)
Leu	21.29(0.13)	29.89(0.25)	16.73(0.13)	24.37(0.07)	15.64(0.13)	24.96(0.22)	11.54(0.33)
Met	12.47(0.09)	14.12(0.23)	7.60(0.43)	12.48(0.11)	8.40(0.07)	N.D.	N.D.
Phe	10.35(0.01)	10.06(0.36)	7.75(0.09)	10.27(0.35)	6.80(0.21)	12.85(0.22)	10.31(0.02)
Ser	9.87(0.15)	12.49(0.28)	7.34(0.09)	10.80(0.06)	7.23(0.08)	20.06(0.49)	5.73(0.06)
Thr	5.96(0.10)	(-1.4)(0.42)	4.00(0.10)	8.15(0.33)	(-1.96)(0.07)	(-16.79)(0.03)	6.97(0.15)
Tyr	12.76(0.27)	14.52(0.02)	9.14(0.07)	12.27(0.23)	8.46(0.046)	N.D.	8.87(0.11)
Val	22.89(0.27)	29.71(0.32)	18.94(0.07	24.74(0.20)	17.05(0.13)	26.45(0.42)	15.18(0.19)
Glu-Phe	17.29(0.34)	20.10(0.33)	10.52(0.29)	15.25(0.12)	11.76(0.10)	13.15(0.35)	5.48(0.28)
TP	2.8(0.85)	3.2(1.08)	1.9(0.41)	2.6(0.70)	2.1(0.48)	2.3(0.56)	1.3(0.20)

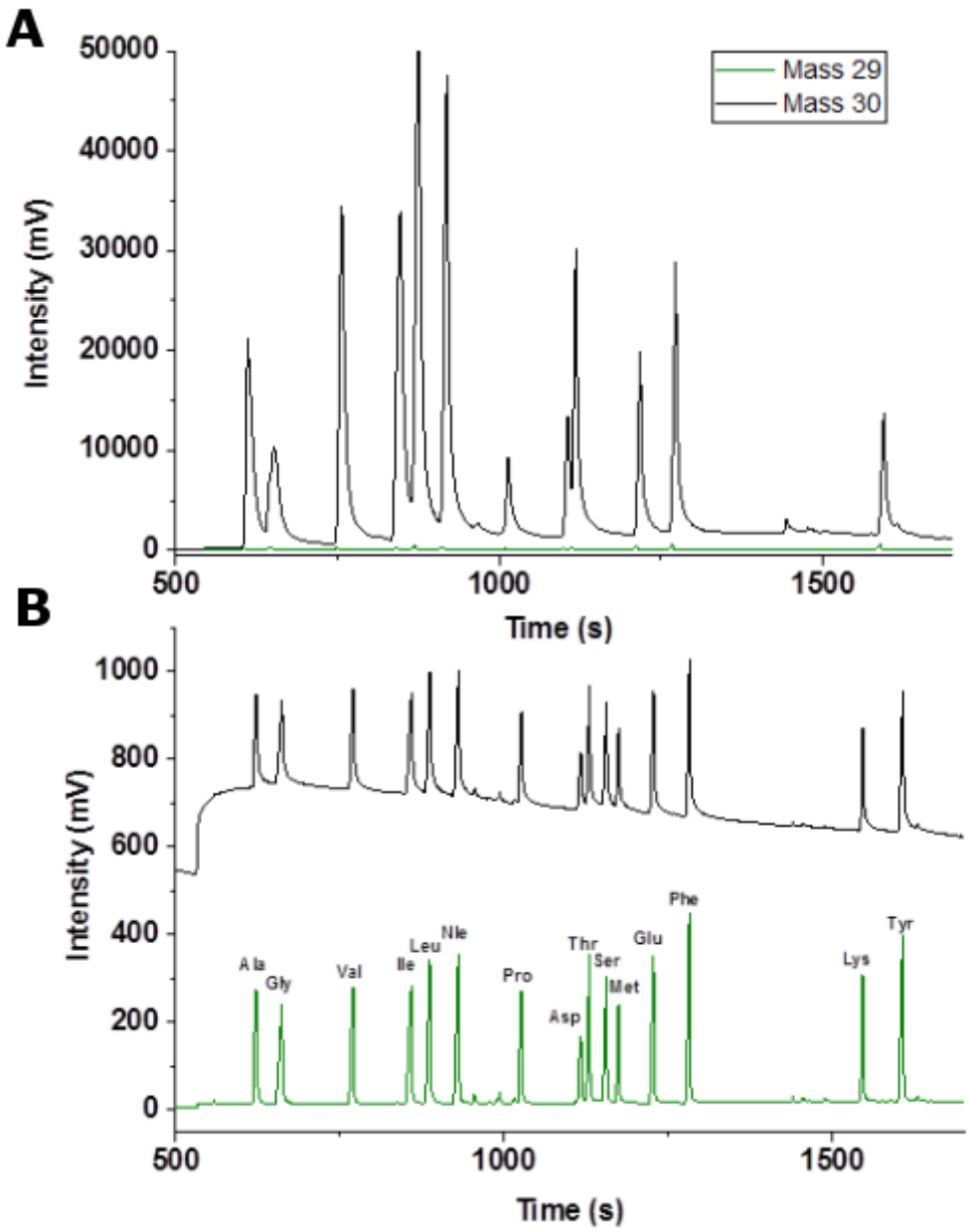

Figure 1: Chromatograms for amino acid standards run immediately after A) oxidation of the combustion reactor on the GC combustion III interface and B) oxidation, backflush and conditioning for the single combined oxidation-reduction reactor and Isolink II interface. Note the difference in y axis scale between the two plots. For acronyms of amino acids see main text.

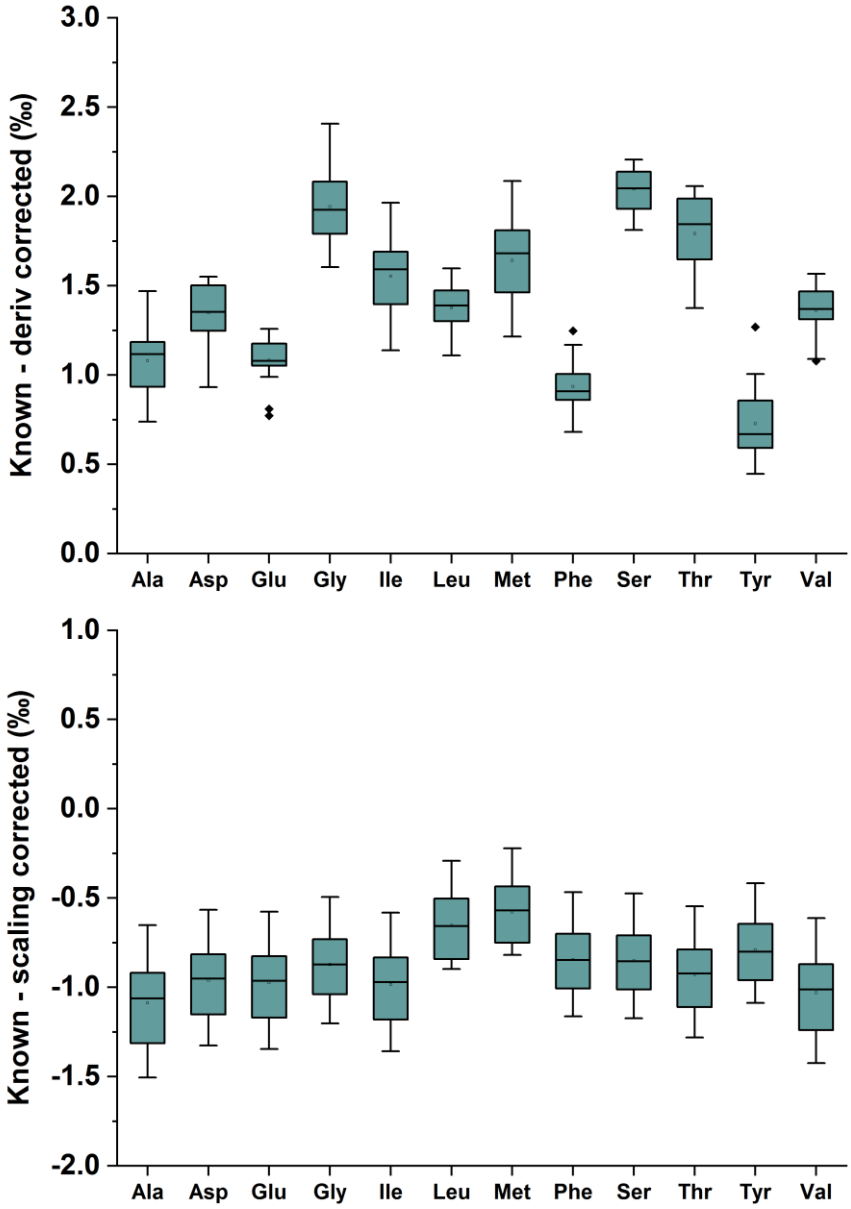

Figure 2: Box plots of measured isotopic offsets for a 12 amino acid standard mixture across 16 daily runs between A) δ15N values measured by EA-irMS for free amino acids and by GC/C-irMS corrected for derivatization and B) δ15NAAi, offsets between known δ15NAA values from EA-irMS analysis and δ15NAA values measured by GC/C-irMS corrected for derivatization and scaled to internationally calibrated compound specific standards. Within the boxplots, black dots are the mean, lines represent the median, boxes represent the upper and lower quartiles, and whiskers represent the 1.5 quartile ranges. Any black diamonds outside of the whiskers are outliers.

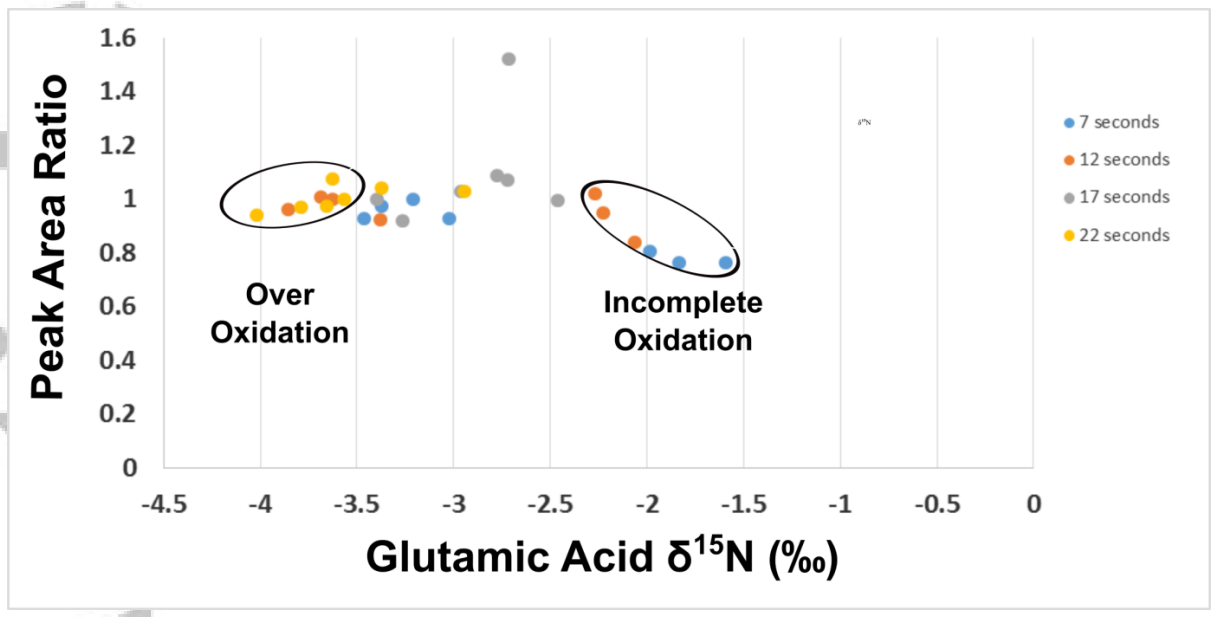

Figure 3: δ15N values of glutamic acid versus peak area ratio for offset standard mix replicates (n=7) with different lengths of seed oxidation. Peak area ratios below 1 indicate incomplete oxidation and coincide with increase in δ15N values (~2 ‰, 7 and 12 second seed oxidations) which worsened through the sequences (marked Incomplete Oxidation, last three replicates of both 7 and 12 second trials, 5 through 7). Additional oxidation resulted in complete combustion as evidenced by the peak areas, but also resulted in decreasing δ15N values with relatively small increases in oxidation times (0.75-1‰, 22 second trial) which decreased precision across the sequence.

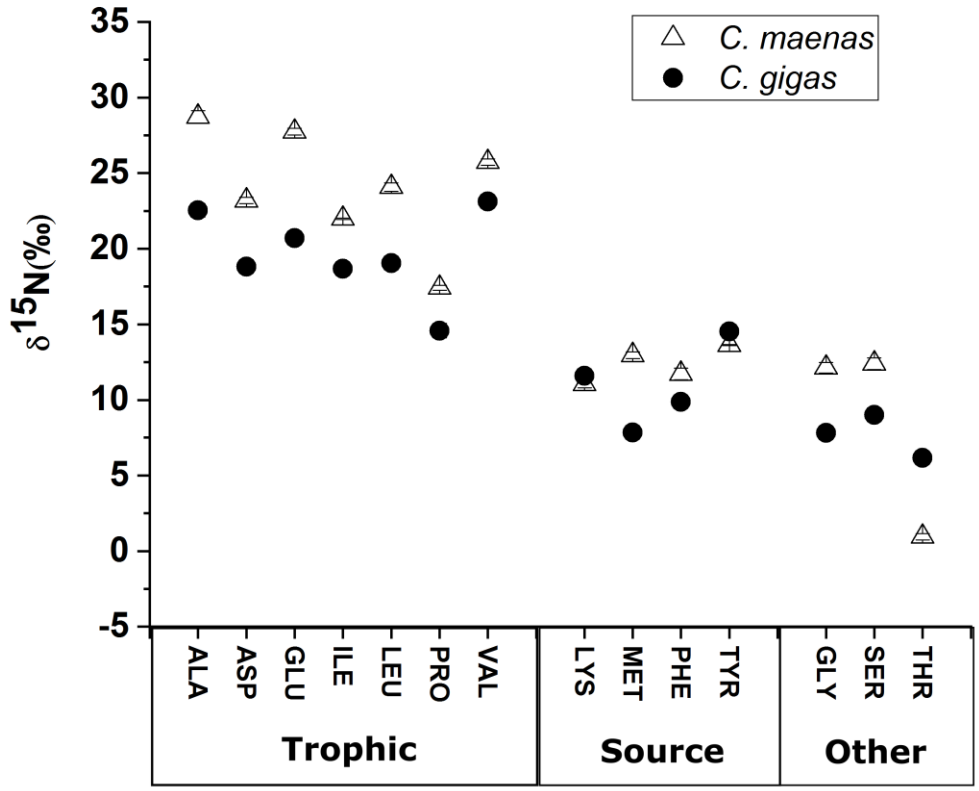

Figure 4: δ15N values for 14 amino acids for European Green Crab (Carcinus maenas) and Pacific Oyster (Crassostrea gigas) assigned to "Trophic", "Source" and "Other" groups based on how they are metabolized. These samples were run in triplicate with a 17 second oxidation using the standards presented in Figure 3. Mean ± SD for triplicate replicates, SD all <0.5 ‰; Supplementary Table 3 (supporting information), some error bars are too small to be seen.

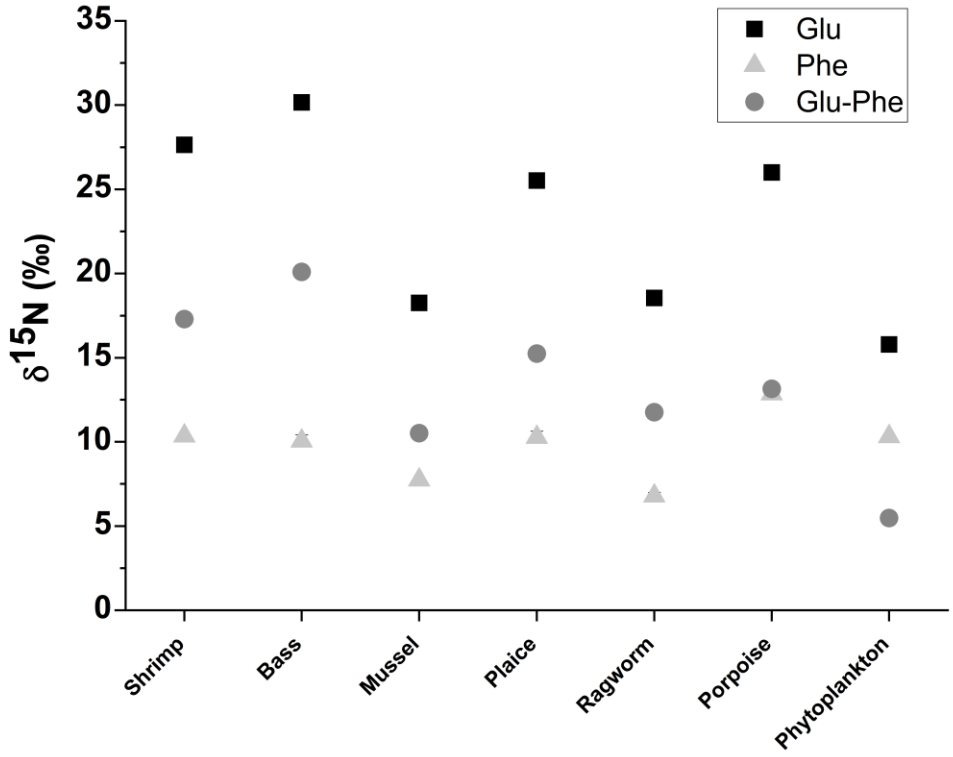

Figure 5: δ15N values of glutamic acid and phenylalanine for 7 samples as well as the difference that is commonly used in the calculation of trophic position. (Mean ± SD of analytical duplicates, error bars are too small to be seen)

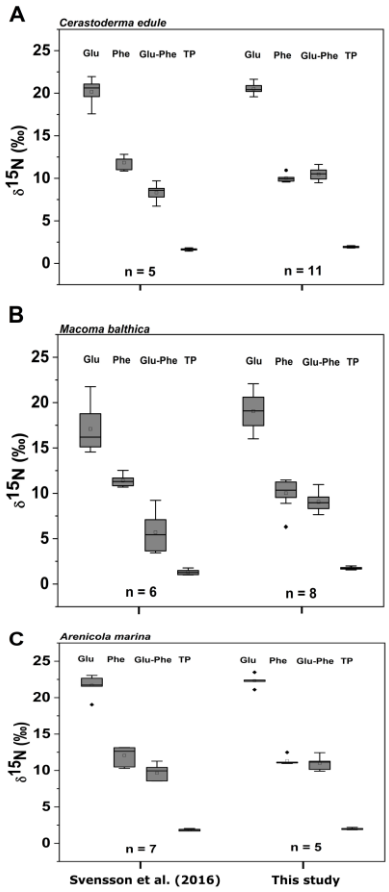

Figure 6: δ15N values for glutamic acid (Glu), phenylalanine (Phe), Glu-Phe, and trophic position (TP) for A) C. edule (common cockle), B) M. balthica (Baltic clam), and C) A. marina (lugworm) analyzed using the method presented in this study and the previously used method (Svensson et al. 2016). Note that TP is unitless and is shown between methods for a comparison of precision provided with the two measurement estimates disregarding the error associated with the trophic discrimination factor (7.6 ± 2.5‰) and β (3.4 ± 0.9) used to calculate TP. Within the boxplot, open squares represent the mean, lines represent the median, boxes represent the upper and lower quartiles, and whiskers represent the 1.5 quartile ranges. Any black squares outside the whiskers are outliers and n refers to number of individuals analyzed.